Journal of Materials Science and Chemical Engineering, 2024, 12, 67-83
https://www.scirp.org/journal/msce
ISSN Online: 2327-6053
ISSN Print: 2327-6045

Tensile Mechanical Behavior and Failure Mechanism of a Plain-Woven SiCf/SiC Composites at Room and Elevated Temperatures

Jianze He[1], Xuefeng Teng[1,2*], Xiao'an Hu[1,2], Xiao Luo[3], Qi Zeng[3], Xueqiang Cao[4]

[1]School of Aircraft Engineering, Nanchang Hangkong University, Nanchang, China
[2]Jiangxi Key Laboratory of Micro Aeroengine, Nanchang, China
[3]Hunan Aviation Powerplant Research Institute, Aero Engine Corporation of China, Zhuzhou, China
[4]State Key Laboratory of Silicate Profound Building Materials, Wuhan University of Technology, Wuhan, China
Email: *tengxf0302@163.com

How to cite this paper: He, J.Z., Teng, X.F., Hu, X.A., Luo, X., Zeng, Q. and Cao, X.Q. (2024) Tensile Mechanical Behavior and Failure Mechanism of a Plain-Woven SiCf/SiC Composites at Room and Elevated Temperatures. *Journal of Materials Science and Chemical Engineering*, **12**, 67-83.
https://doi.org/10.4236/msce.2024.124006

Received: March 15, 2024
Accepted: April 22, 2024
Published: April 25, 2024

Abstract

Ceramic matrix composites (CMCs) are the preferred materials for solving advanced aerospace high-temperature structural components; it has the comprehensive advantages of higher temperature (~1500˚C) and low density. In service environments, CMCs exhibit complex damage mechanisms and failure modes, which are affected by constituent materials, meso-architecture and inhere defects. In this paper, the in-plane tensile mechanical behavior of a plain-woven SiCf/SiC composite at room and elevated temperatures was investigated, and the factors affecting the tensile strength of the material were discussed in depth. The results show that the tensile modulus and strength of SiCf/SiC composites at high temperature are lower, but the fracture strain increases and the toughness of the composites is enhanced; the stitching holes significantly weaken the tensile strength of the material, resulting in the material is easy to break at the cross-section with stitching holes.

Keywords

Plain-Woven, SiC_f/SiC Composites, Damage and Failure Analysis, Stitching Hole

1. Introduction

SiCf/SiC Ceramic Matrix Composites (CMCs) are the key materials for the hot end components of next-generation aero-engines [1]. The pre-turbine tempera-

ture of the first domestic large bypass ratio turbofan engine is about 1600˚C, far exceeding the service limit of single crystal and intermetallic superalloy (1100˚C) [2] [3]. Compared with traditional metal materials, the density of SiCf/SiC CMCs is only 1/3, the temperature resistance is improved by 20%, and its strength can be maintained at 1300˚C - 1400˚C without cooling. With thermal barrier coating, SiCf/SiC can be used for a long time at 1600˚C without cooling [4]. The application of CMCs in the aerospace can effectively reduce structural weight, reduce cooling requirements, and significantly reduce oil consumption and NOx and CO emissions [4], which are ideal materials for hot end components of advanced aero engines in the future, and also an important research direction for technical breakthroughs in the aerospace field [5] [6].

With the development of material science and the improvement of the demand for material performance in aerospace, CMCs have accumulated nearly 30 years of installed use/application experience on aero-engine low-bearing stator components [4], gradually completed the verification of tail nozzle, turbine shroud, flame tube and other components, and are carrying out application research on high-bearing rotor components (such as turbine blades). In terms of CMCs rotor components, Liu prepared the SiCf/SiC integrated turbine blisk, passed 1000 0-Max-0 ground machine test, and successfully completed the first flight test, verifying the feasibility of applying CMCs structure to rotor components [7].

In the design of integral turbine blisk, due to the axisymmetric structural characteristics of the integral bladed disk, the two-dimensional polar braiding and Z-direction stitching technology are usually used to prepare the integral bladed disk structure [7] [8]. Two-dimensional polar braiding is the preparation process of interlacing and laying the fiber bundles along the radial and circumferential directions of the blisk, and laminating the multi-layer fiber cloth along the Z/axial direction. In the part of the blisk, it can be approximated as two-dimensional laminated woven composite material [7] [8] [9] [10]. Many studies have been carried out on two-dimensional SiC/SiC composites at home and abroad: Morscher *et al.* [11] showed that cracking stress is related to the maximum defect area and fiber volume fraction of two-dimensional (2D) SiC/SiC composites; Li [8] studied the in-plane shear properties of two-dimensional braided SiC/SiC composites through unidirectional and cyclic loading and unloading in-plane shear tests; Han [9] develped a multi-scale analysis for turbine guide vanes made of 2D braided SiCf/SiC composites in high-cycle fatigue (HCF) regime; Wang [10] [12] investigated the damage evolution behavior of the plain-woven SiC/SiC under tensile and fatigue loads at room temperature using acoustic emission technology, and found that the material damage is closely related to loading process; Song [13] conducted a three-point bending test using AE system and DIC technology to evaluate the mechanical properties of two-dimensional (2D) SiCf/SiC braided composite materials and characterized the mechanical behavior of the two-dimensional braided SiCf/SiC composite materials in various ways; Hu [14] carried out experimental and modal analysis research on the vibration characte-

ristics of two-dimensional braided SiC/SiC composites; Zhang [15] studied the microstructure and damage evolution process of two-dimensional plain woven SiC cmposites under load using X-ray in situ CT and deep learning image processing algorithm; Han studied the stress oxidation behavior of 2D CVI-SiC/BN/SiC composites at intermediate temperatures (800˚C) and found that fiber degradation and interface defects caused by component oxidation led to local fiber failure and final fracture of the composite materia And some scholars have studied the effects of heat treatment [16] and gas environment [17] on the properties of SiC composites.

The creation of CMC parts usually uses two-dimensional diagonal layers of planar or woven fiber bundles, with interface phases deposited onto the fibers between the creation of the preform [18]. Subsequently, various penetration based methods are used to fully penetrate the matrix into the thick cross-section, but more porous internal areas are also generated. Since 2D CMC materials are always weak in the transverse direction and prone to "splitting" faults, the fabricators introduced stitched fibre bundles in the vertical direction to solve this problem [19]. However, removing the sutured fiber bundles will leave sutured through-holes in the sample, which becomes the main internal defect of CMCs materials.

However, there is relatively little research on sutured holes. The present paper focuses on the tensile properties and failure of coated plain-woven SiCf/SiC composites at room and high temperatures. The experimental study was carried out to obtain the basic mechanical behavior and properties, the negative effect of stitching hole on the tensile strength and failure of the material were investigated, which is helpful to design CMC materials with higher strength and better mechanical properties.

2. Materials and Experimental Procedure

2.1. Material and Specimens

The material studied in this paper is a two-dimensional plain-woven SiCf/SiC composite, using the domestic third generation SiC fiber, the fiber diameter is about 11 μm, and the fiber modulus and tensile strength are 270 GPa and 3 GPa, respectively. The material preparation process is as follows: Firstly, the SiC fiber bundle is braided into the fabric preform, and the BN interface is deposited on the fiber surface of the fabric preform. The BN interface deposition temperature is 900˚C - 1000˚C, the deposition time is 72 h, and the thickness of the interfacial layer is 200 - 300 nm. Then, the SiC matrix was deposited by CVI process, trichloromethyl silane was used as the precursor of SiC, and H2 and Ar were used as dilution gas. The gas was introduced into the reaction zone of the deposition furnace by bubble method. The deposition temperature was 1000˚C - 1100˚C, and the deposition time was 40 - 48 h. In order to improve the density of SiC matrix, the above SiC matrix deposition process was repeated eight times. The SiCf/SiC composites prepared by this method have a density of 2.5 g/cm^3 and a porosity of 5%.

The test specimens of the plain-woven SiCf/SiC composite were cut from a large composite sheet, with the desired size and cutting direction according to the test method ASME C1359 [18]. After cutting from the composite sheet, atmospheric plasma spraying was used to prepare environmental barrier coating (EBC) on the surface of samples at high temperature. The structure of EBC consisted of three layers, namely Si/Yb_2SiO_5/La_2O_3-Al_2O_3, and the coating thickness was 0.2 mm. Figure 1 shows the size and the CT scanning image of the plain-woven SiCf/SiC composites. It can be seen that the material has a two-dimensional plain-woven structure, and there are lots of pore defects in the interweaving parts of fiber bundles inside the material.

2.2. Experimental Process

The in-plane tensile tests were carried out by an electronic universal testing machine INSTRON 8872, the maximum load is 25 kN, the load and displacement control precision are within 0.5%. In the high temperature tensile test, the cold end is clamped, and a high temperature environmental furnace is used to heat the test section of the specimen. When the temperature of the high temperature furnace reaches the test temperature, hold the specimen for 20 minutes to make the temperature of the test section uniform and stable, and then start the test. Figure 2 shows the details of the tensile test device. According to the operating manual the in-plane tension test for coated specimens were conducted at 1200˚C and 1350˚C.

In this paper, the high temperature furnace shown in Figure 2(a) was used for tensile test at 1200˚C. Asbestos was used as insulation filler to seal and keep

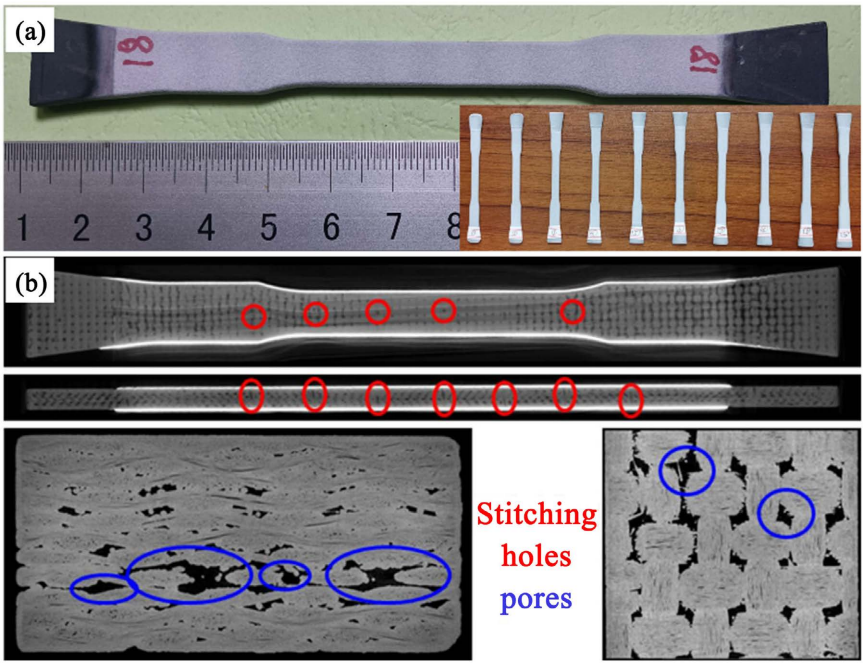

Figure 1. (a) Type and size of the SiC_f/SiC specimen, with EBC in white section; (b) CT images of the specimen, with stitching holes and pores in the specimen.

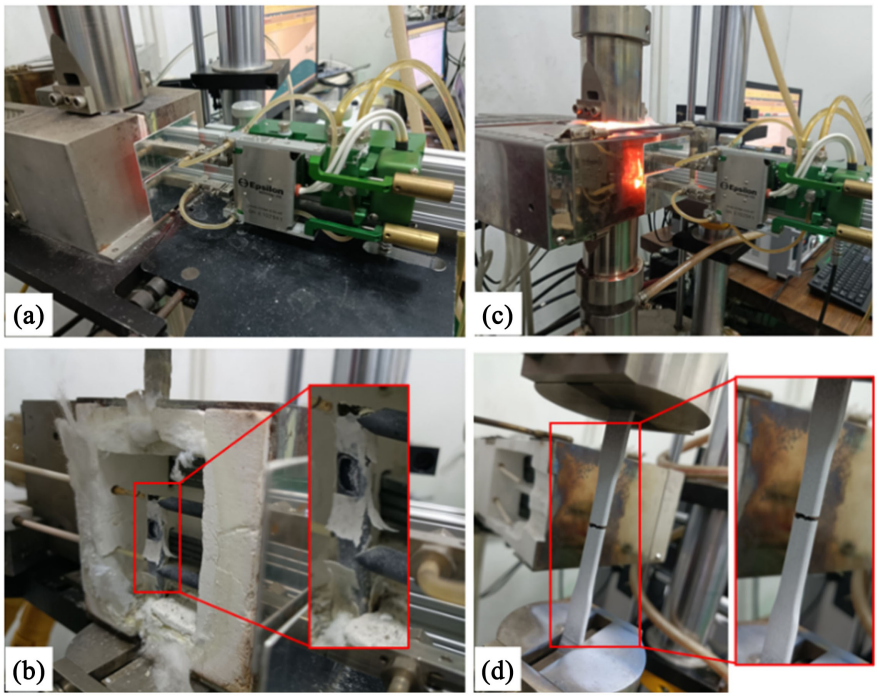

Figure 2. High temperature tensile test of SiC_f/SiC composites: (a) 1200˚C high temperature environment furnace; (b) 1200˚C EBC peeling; (c) 1350˚C high temperature environment furnace; (d) 1350˚C intact EBC.

warm the high temperature furnace. The test results show that asbestos is unstable at 1200˚C and reacts with the EBC coating on the surface of SiC_f/SiC material, causing the coating to fall off locally (**Figure 2(b)**). Therefore, a new, uncontaminated high temperature furnace (**Figure 2(c)**) was used at 1350˚C, and alumina fiber felt with better high temperature resistance and stability was used to seal and keep warm the high temperature furnace. No coating peeling was found on the surface of the samples after the test (**Figure 2(d)**).

3. Results and Discussion

3.1. Tensile Mechanical Behavior

In this paper, the in-plane tensile mechanical properties of SiCf/SiC composites were tested at room and elevated temperatures. Uncoated specimens were used for tensile tests at room temperature. The specimens were No. RT-1, RT-2, RT-3 and RT-4. The high-temperature tensile test was for coated specimens, whose numbers were 1200˚C-1, 1200˚C-2, 1200˚C-3, 1200˚C-4, and 1350˚C-1, 1350˚C-2, 1350˚C-3, 1350˚C-4, respectively.

3.1.1. Tensile Mechanical Properties at Room Temperature

Figure 3 shows the in-plane tensile stress-strain response of SiCf/SiC composites at room temperature. As can be seen from the figure, the tensile deformation process of the specimen can be divided into three stages. The first stage: At the initial stage of loading, the stress-strain response of the specimen is linear, and

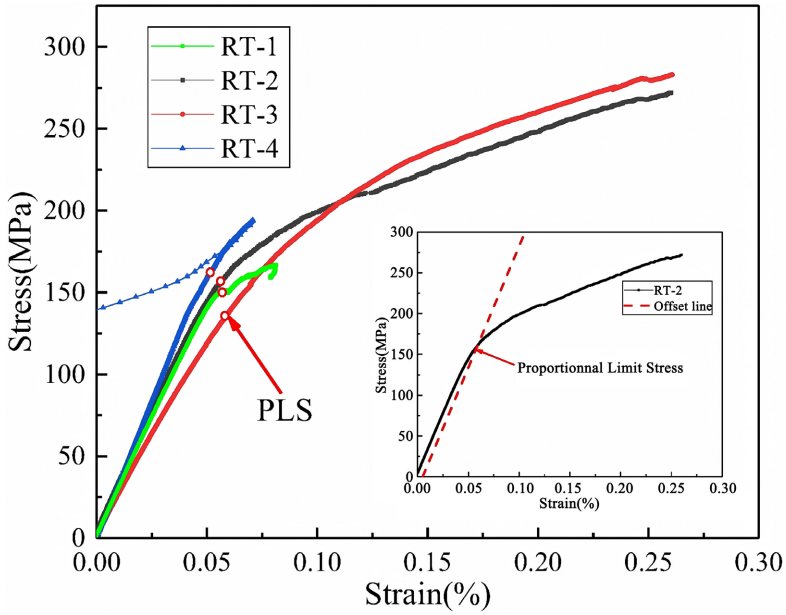

Figure 3. In-plane tensile stress-strain curves of SiC_f/SiC composites at room temperature.

the tensile strain basically increases linearly with the increase of load. Stage 2: The strain offset method is adopted, and the stress corresponding to the inelastic strain of 0.005% is taken as the proportional limit stress (PLS) of the material. When the stress of the material reaches the proportional limit stress, the stress-strain curve enters the nonlinear stage with the continuous increase of the load. At this time, crack initiation and crack propagation begin to occur in the defective parts of the matrix inside the material, leading to the gradual decrease of the macroscopic stiffness of the material. Stage 3: The matrix crack inside the material reaches saturation, and the external load is mainly borne by the continuous fiber; With the increase of applied load, the macroscopic tangential stiffness of the material basically remains unchanged, and the stress-strain curve increases linearly with a small slope (specimen RT-2 and RT-3), indicating that no obvious fiber fracture occurs at this stage, and the dispersion of SiC fiber fracture strength is small. Before the fracture of the sample, the stress-strain curve fluctuated slightly (specimen RT-2 and RT-3), indicating that some fibers fractured. Subsequently, the true stress of the remaining bearing fiber bundle reached the fracture strength of the fiber bundle, and the fiber bundle broke, and the specimen lost its bearing capacity.

The elastic modulus, proportional limit, tensile strength and fracture strain of the material were calculated according to the stress-strain curve, as shown in Table 1.

It can be seen from the test curve and test results that the mechanical properties of SiCf/SiC composites have a certain dispersion, especially the strength properties (such as proportional limit, fracture strength, fracture strain) have a greater dispersion. The dispersion of SiCf/SiC composites comes from meso/micro-scale

Table 1. In-plane tensile properties of SiCf/SiC composites at room temperature.

Specimen number	Elastic modulus (GPa)	PLS (MPa)	Strength (MPa)	Fracture strain (%)	Stitching hole
RT-1	293	150.74	175.14	0.078	None
RT-2	297.36	160.25	271.94	0.260	None
RT-3	252.03	135.16	282.92	0.261	1
RT-4	339.7	164.44	194.12	0.071	1

manufacturing defects, such as pores, microcracks, etc. Under external load, the crack initiation and propagation of the fabrication defects lead to the reduction of the bearing capacity of the materials to different degrees, and the stress-strain response of the materials shows the characteristics of dispersion. The elastic modulus of the material is a global average. Although the damage evolution process and damage degree of different specimen are different, the elastic modulus of the material is less dispersed macroscopically after the global average of the whole specimen. The strength performance of materials mainly depends on the most dangerous defects in the specimen. Materials containing serious manufacturing defects have low damage tolerance, and the defects will evolve into more serious damage under lower loads, resulting in the failure of materials. For materials without serious manufacturing defects, the damage evolution process is relatively slow, resulting in higher strength properties.

3.1.2. Tensile Mechanical Properties at Elevated Temperatures

According to the typical service temperature of SiCf/SiC composites, the in-plane tensile mechanical properties of SiCf/SiC composites were tested at 1200˚C and 1350˚C, and the stress-strain curves were shown in **Figure 4**. As can be seen from the figure, SiCf/SiC composites also exhibit obvious three-stage stress-strain relationship at high temperature. Among them, the stress-strain curves of specimens 1200˚C-1 and 1200˚C-2 show obvious fluctuation, which is due to the arc transition of the end loading site of specimens 1200˚C-1 and 1200˚C-2 (see **Figure 1**), resulting in slight relative sliding or rotation between the specimen and the fixture during the loading process. Due to the displacement-controlled loading method adopted in the test process, the small slip of the specimen causes the sudden change of the load of the sample, which leads to the fluctuation of the stress and strain. However, for other high temperature tensile specimens, the loading position of the specimen is stable in contact with the loading surface of the fixture, and no obvious stress-strain curve fluctuation is observed. The mechanical properties of the specimens at high temperature are shown in **Table 2**.

Off gauge, the fracture cross-section of the specimen is outside the test segment.

With the increase of ambient temperature, the mechanical properties of SiC fibers decrease first and then increase, which indicates that SiCf/SiC composites can give full play to the excellent properties of fibers in some high temperature

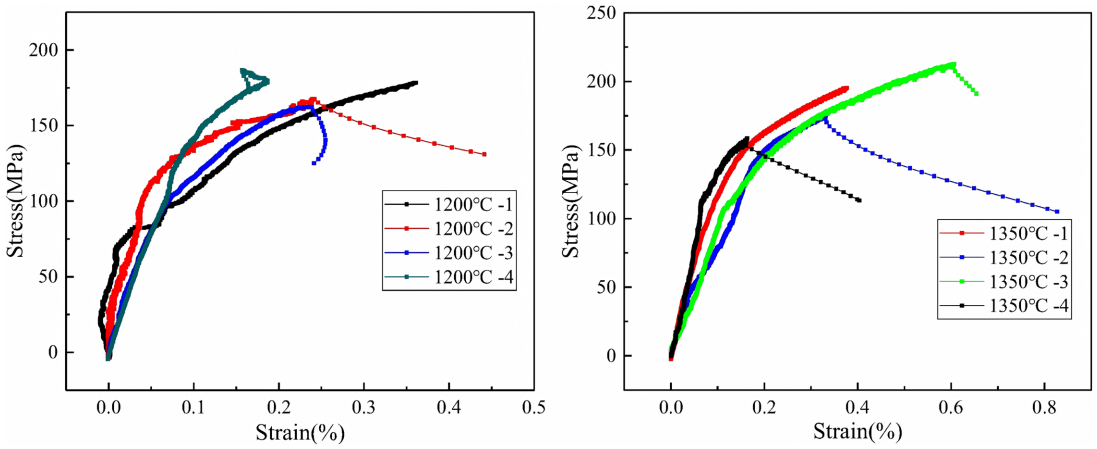

Figure 4. In-plane tensile stress-strain curves of SiC_f/SiC composites at elevated temperatures.

Table 2. In-plane tensile properties of SiC_f/SiC composites at elevated temperatures.

Specimen number	Elastic modulus (GPa)	Strength (MPa)	Fracture strain (%)	Stitching hole
1200˚C-1	179.2	178.2	0.35	1
1200˚C-2	201.3	167.5	0.25	2
1200˚C-3	199.4	186.5	0.18	2
1200˚C-4	145.4	162.2	0.25	1
1350˚C-1	129.2	195.29	0.37	Off gauge
1350˚C-2	66.6	175.40	0.82	1
1350˚C-3	93.2	212.68	0.65	None
1350˚C-4	158.2	158.50	0.42	1

environments. The results show that the change of tensile strength of SiC fibers is related to the change of fiber microstructure and orientation. The evolution of fiber microstructure in SiC fibers varies with temperature and can be divided into four stages: intermolecular crosslinking (≤600˚C), basically inorganic transformation (600˚C - 800˚C), completely inorganic transformation (800˚C - 1300˚C) and crystallization and redistribution of the structure (1300˚C - 1800˚C). With the increase of inorganic degree, the tensile strength of fiber increases gradually. In the stage of crystal rearrangement, the fiber grains gradually increase and start to rearrange, and its tensile strength gradually decreases [2]. The experimental results of this paper also show that the tensile strength at 1350˚C (185.5 MPa) is slightly higher than that at 1200˚C (173.6 MPa), but the elastic modulus at 1350˚C is lower.

3.2. Failure Analysis

Because of the special meso-structure and properties of SiC fiber, the failure process of plain-woven SiCf/SiC composites is very different from that of metal materials, including crack initiation, propagation, fiber bridging, fiber fracture,

fiber pulling out, etc. Due to the complex meso-three-dimensional structure and preparation process of the material, there will be congenital manufacturing defects with different shapes and sizes in the matrix area, such as pores and microcracks. During the initial loading, microcracks will occur in the defects inside the matrix. Due to the small load, microcracks only exist in part of the matrix, which corresponds to the linear stage of the stress-strain curve. As the load continues to increase, the microcracks gradually increase and expand until the matrix cracks in the material reach saturation, which shows a nonlinear stage on the stress-strain curve. When the matrix cracks are saturated, the external load is mainly borne by the fiber bundle. With the further increase of the external load, interface debonding, fiber fracture, fiber pulling out and other phenomena occur, which eventually lead to the fracture failure of the specimen and the loss of the bearing capacity of the material.

3.2.1. Fracture Analysis of Specimens

This paper makes an observation of the fracture using a tungsten filament scanning electron microscope made by Hitachi, Japan. According to the tensile stress-strain curve, when the nominal stress is lower than the PLS, no macroscopic damage occurs inside the sample, and it is in the linear elastic stage. When the stress continues to increase beyond the PLS, the stress-induced crack in the matrix will extend to the fiber/matrix interface. Due to the stress release effect of the interface, the crack will deflect at the interface and expand along the interface layer. Different interface strength would lead to different results: When the interfacial bonding strength is weak, the fiber will debond and the crack will expand along the fiber/matrix interface. Due to the release of part of the energy, the fiber shows a good strength performance and the toughening effect, until finally the fiber fractured and is pulled out from the matrix. When the interface bonding strength is strong, the fiber/matrix interface would not debond, the crack extends into the fiber through the interface, the energy is not released, the crack passes through the fiber and leads to the fiber bundle fracture, without fiber pulling out. In the materials studied in this paper, most of the fibers are strongly bound to the matrix, while few fibers are weakly bond, so the fracture is macroscopically flat, only a few fibers are pulled out from the matrix, and the fiber pulling length is short.

The tensile failure of composites is related to the failure of matrix, interface and fiber. The fracture morphology of the 2D plain-woven SiCf/SiC composites is shown in **Figure 5**, which mainly has the following failure characteristics: 1) A large number of fibers are pulled out or the whole fiber bundle is pulled out, and the fracture surface of the sample presents uneven characteristics; 2) The crack propagation path mainly extends along the inherent defects of fiber/matrix, fiber bundle/fiber bundle interface, such as weak areas, unfilled areas and pores. 3) The fiber fracture surface shows the characteristics of mirror surface, brittle fracture, and step shape.

As can be seen from **Figure 1**, there are many meso-pores in the interlacing

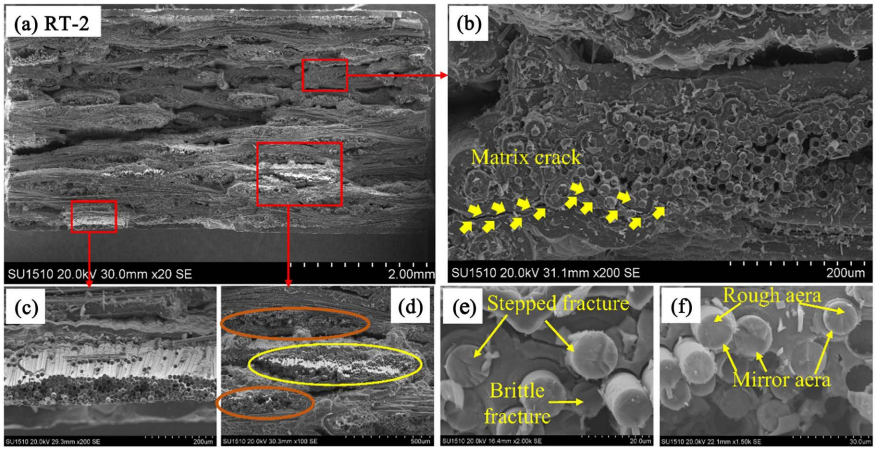

Figure 5. Tensile fracture morphology at room temperature: (a) Overview of the fracture; (b) Fiber bundle fracture and matrix crack propagation; (c) Fiber bundle pull-out and fracture; (d) Fiber bundle fracture morphology; (e) and (f): Fiber fracture.

zone of the fiber bundles of SiCf/SiC composites. When the fracture occurs in the part with more pores, there is no matrix connection between the fiber bundles, and the fiber bundles are broken and damaged respectively, resulting in uneven fracture of the fiber bundles and not in the same plane, as shown in **Figure 5(a)**. **Figures 5(b)-(d)** are the SEM images of the fiber bundle fracture. It can be seen that the fiber volume fraction in the fiber bundle is high, the fibers are closely arranged, and the fiber/matrix interface strength in the fiber bundle is relatively strong. In addition, fewer meso-matrix cracks were observed in the material (**Figure 5(b)**), which also indicates that the interface strength was relatively high, and interface cracking and debonding rarely occurred. By observing the microscopic fiber fracture, it can be found that the fiber fracture has obvious brittle fracture characteristics, such as brittle fracture, mirror area and step fracture formed by multi-source crack propagation (**Figure 5(e)** and **Figure 5(f)**). Fiber fracture caused by fiber strength has obvious mirror fracture, and there are obvious rough and mirror areas on the surface of the fracture, as shown in **Figure 5(f)**, indicating that fiber fracture is caused by its own defects and has nothing to do with matrix crack propagation. When the crack extends to the higher strength of the fiber/matrix interface, the crack penetrates and severs the fiber. In this case, the fiber fracture showed obvious brittle fracture characteristics, as shown in **Figure 5(e)**. There are usually multiple crack growth sources around a single fiber, including primary crack and secondary crack. The stepped fracture of some fibers is the result of multiple crack growth. When the crack in a single fiber expands to a certain extent, the crack propagation is delayed due to the local stress release. Then, under the stress redistribution mechanism, the fiber is reloaded, and the crack further expands inside the fiber until the fiber fractures. Therefore, the fracture appears step characteristics (**Figure 5(e)**).

At high temperature, the mechanical properties of materials degrade to a certain extent. The elastic modulus and failure strength of materials at high temperature decrease significantly, but the fracture strain increases significantly.

EBC coating can effectively prevent the oxidation of SiCf/SiC materials in high temperature environment. Through SEM observation and analysis of high temperature specimen fracture, no obvious oxidation characteristics were found, and the short-term tensile mechanical properties of materials in high temperature environment are less affected by high temperature oxidation. The SEM images of the fracture of coated specimens at high temperature are similar to those of tensile tests at room temperature (**Figure 6(a)**). Most areas show the overall fracture of fiber bundle (**Figure 6(b)**), while a few areas have fiber pulling out (**Figure 6(c)**), and the length of pulling out is relatively short. The fiber section also presents a stepped fracture section. Compared with the room temperature fracture, the proportion of fibers pulled out in the fiber bundle at high temperature was larger, and the length of fibers pulled out was slightly longer, but it was not obvious. This is because the bonding strength of BN interface decreases to a certain extent at high temperature, which increases the proportion of fiber debonding and fiber pulling out. However, the pull-out length of the fibers is still short, indicating that the reduction of the strength performance of the BN interface is not significant.

According to the tensile stress-strain curve at room temperature, RT-1 and RT-4 specimens have low fracture strain and small fracture strength, and fracture failure occurs before or after entering the third stage. The fracture strain and fracture strength of RT-2 and RT-3 specimens are relatively high, and there is a relatively complete stress-strain third stage. By observing the fracture surface of specimens (**Figure 7**), it can be seen that the fracture of specimens RT-1 and

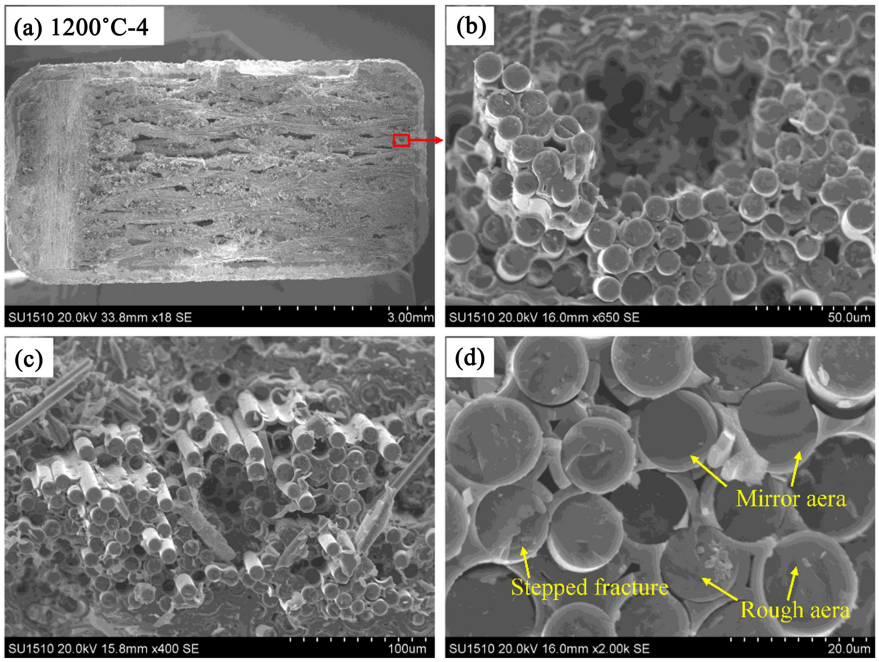

Figure 6. (a) SEM image of specimen fracture of tensile test at high temperature; (b) Integral breakage of the fibre bundle; (c) Fibre extraction in a few areas; (d) the majority of the region shows an overall fracture of the fibre bundle.

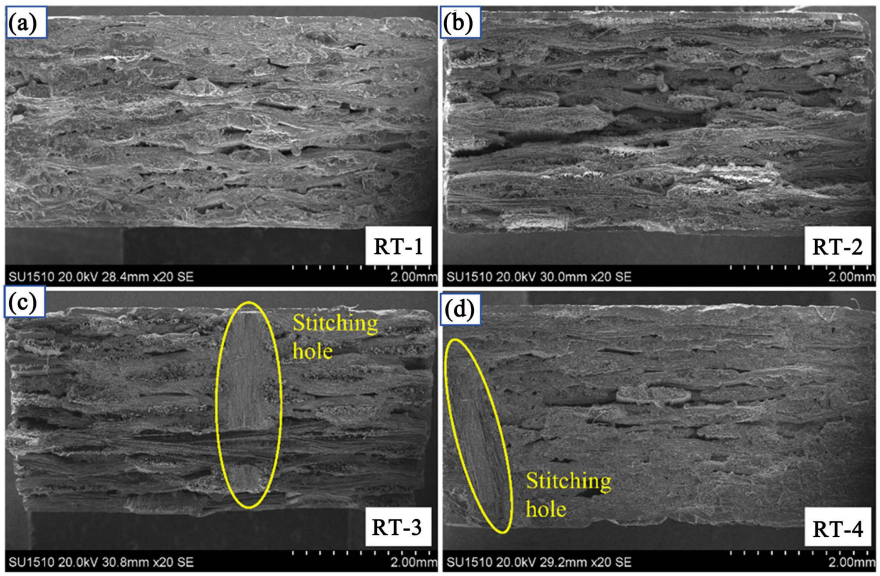

Figure 7. (a) Overall fracture at room temperature; (b) delamination of fibres; (c) Presence of stitching hole; (d) Presence of oblique suture holes.

RT-4 is relatively flat, and the fiber bundle is basically broken in the same plane. However, the fiber bundles of specimens RT-2 and RT-3 were broken at different planes, and the fiber bundles had pull out lengths. Similar to the crack propagation in the fiber bundle, when the meso-matrix crack extends to the surface of the fiber bundle, the deflection or penetration of the matrix crack will also occur according to the different bonding strength of the meso-matrix/fiber bundle interface. The matrix crack deflected on the surface of the fiber bundle, resulting in fiber bundle debonding, which was conducive to releasing the energy at the crack tip and improving the toughness and fracture strength of the material. The sample fracture showed obvious fiber bundle pulling out characteristics, as shown in RT-2 and RT-3 in **Figure 7**. If the interfacial binding strength of the matrix/fiber bundle is high, the matrix cracks easily pass through the fiber bundle, resulting in relatively flat fracture of the sample (**Figure 7** RT-1 and RT-4), and the toughness, fracture strength and fracture strain of the material are low.

3.2.2. Effect of Stitching Hole on Tensile Strength

The SiCf/SiC composite studied in this paper is a two-dimensional plain-woven composite, and the fabric preform is composed of multilayer plain-woven layering stacked along the thickness direction. In order to fix the relative position of each layer and compacted the material along the thickness direction during the matrix impregnation process, sutures were used to stitch the fabric preform along the out-of-plane direction before the matrix impregnation, and the sutures were removed after the impregnation. Therefore, there are random distribution of stitching holes in the SiCf/SiC specimen (as shown in **Figure 1** and **Figure 7**), the effective bearing area of the stitching hole cross-section decreases, the stress concentration generated by the stitching hole makes the real stress at the edge of the hole increase significantly, resulting in the nominal strength of the specimen

decreases.

By observing the fracture of tensile specimens at room temperature and high temperature, stitching holes were found in most fracture sections of specimens, as shown in Table 1 and Table 2. Some fracture sections also have two stitching holes, indicating that the existence of stitching holes would reduce the bearing capacity of materials. However, due to the large dispersion of mechanical properties of SiCf/SiC composites, the influence of stitching hole on the strength of specimens is not obvious in the test results. For example, in tensile specimens at room temperature, the fracture strength of specimen with stitching hole is not the lowest. However, with the increase of test temperature, the weakening effect of stitching hole on the strength performance of the specimen is gradually significant. For example, at 1350˚C, the fracture strength of the specimen with stitching holes is low.

There are three main reasons why stitching holes weaken the strength property of the material: 1) Stitching holes cause the interruption of local continuous fibers and reduce the effective bearing fiber bundle/bearing area (as shown in Figure 8); 2) Stitching holes pass through the middle of the fiber bundle and through the thickness direction of the specimen (Figure 8), which would weaken the performance of the fiber bundle and cause local stress concentration, resulting in the weak area of the specimen and easy to become the crack source/failure source; 3) The stitching hole accelerates the oxidation process of the matrix/fiber near the hole, weakening the mechanical properties of materials near the stitching holes. Stitching holes have a non-negligible weakening effect on the strength properties of materials, so that most of the failure of materials originated from stitching holes, and the proportion of failure caused by stitching holes is larger in high temperature environment.

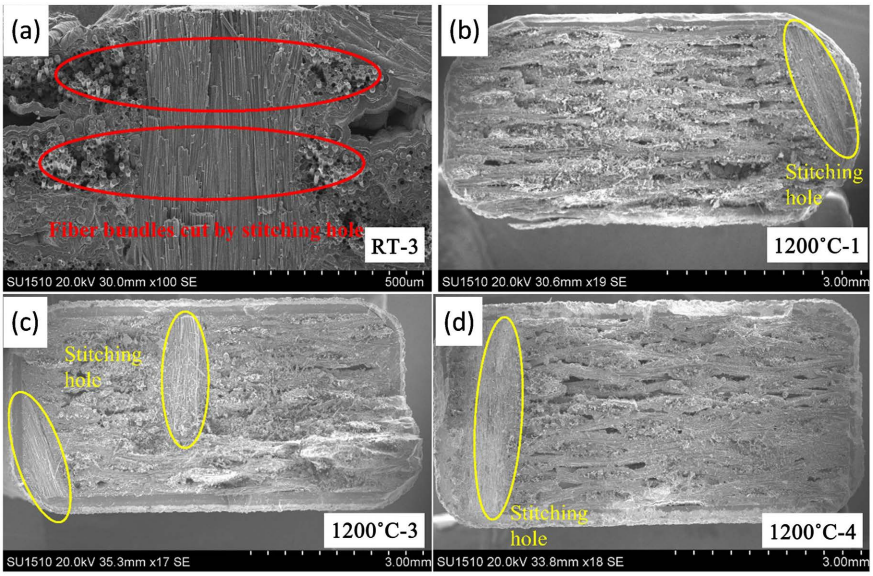

Figure 8. (a) Fiber bundles cut by stitching hole; (b) Diagram of stitching holes cutting continuous fiber bundles; (c) Presence of many suture holes; (d) large stitching hole.

Figure 9(a) and Figure 9(b) shows the SEM images of stitching holes at specimen 1200˚C-2 and 1200˚C-3 fracture sections. As can be seen from the figure, the surface of the stitching hole of the specimen 1200˚C-2 has obvious oxidation characteristics, while no oxidation phenomenon is found in the internal section of the specimen. No oxidation characteristics were observed on the surface and internal section of the suture hole at 1200˚C-3. Figure 9(c) shows the elemental analysis of the local region of the specimen 1200˚C-2 stitching hole. There are oxygen (O), silicon (Si), molybdenum (Mo), ytterbium (Yb) and lanthanum (La) in the oxidation region, indicating that the oxidation reaction between SiC and oxygen generates SiO_2 attached to the surface of the material, and Yb and La elements are components of the EBC coating. It is shown that some EBC coating materials enter the stitching hole and adhere to the surface of the stitching hole during the preparation of the coating on the specimen surface. When the EBC anti-oxidation coating on the specimen surface is relatively dense, it is difficult for oxygen to enter the inside of the material, and no oxidation reaction occurs in the inside of the specimen and on the surface of the stitching hole (1200˚C-3). If the EBC anti-oxidation coating on the specimen surface is relatively loose or thin, inert oxidation may occur inside the specimen and on the surface of the stitching hole, and SiO_2 would generate (1200˚C-2) late (Heading 4).

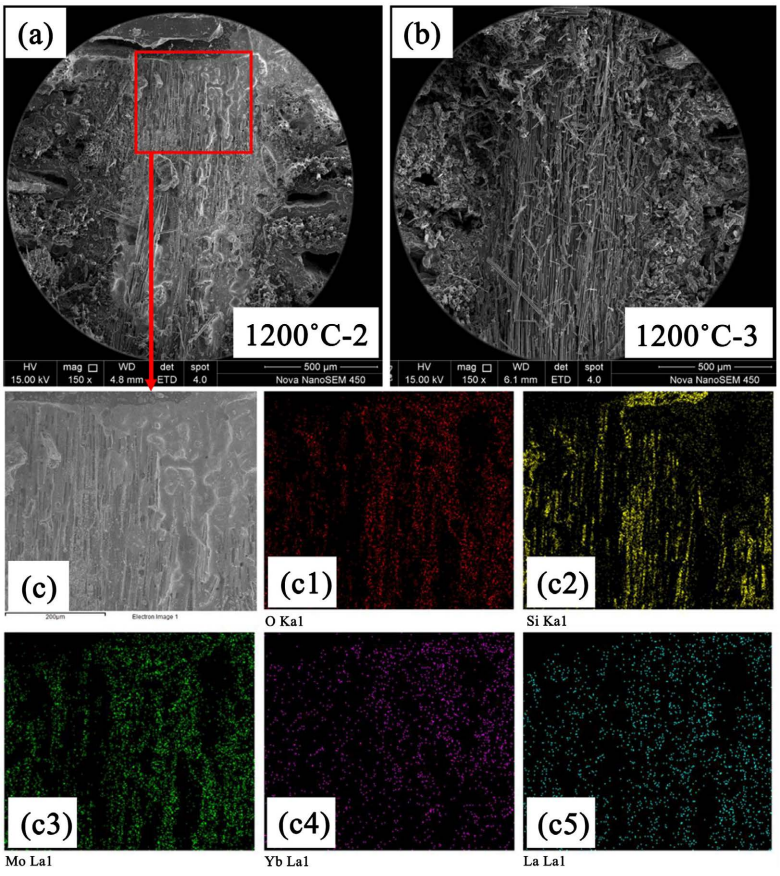

Figure 9. Electron microscopic images ((a) and (b)) and elemental analysis (c) of specimens 1200˚C-2 and 1200˚C-3 fracture stitching holes.

According to the EBC coating preparation process, the EBC coating of SiCf/SiC specimen is composed of three layers. La_2O_3-Al_2O_3 and Yb_2SiO_5 layers can well protect the matrix and fiber inside the material, and increase the oxidation resistance of the material. However, the thermal expansion coefficient and elastic modulus of La_2O_3-Al_2O_3 and Yb_2SiO_5 are quite different from that of SiC, and cannot bond well with CMCs. Therefore, Si is used as the bonding layer, which has good adhesion and thermal expansion matching performance.

Figure 9(a) and Figure 9(c) show the surface oxidation of specimen 1200˚C-2 at the entrance of the stitching hole, and partial surface melting was observed. The element analysis showed that there were more EBC coating elements in this region, indicating that during the preparation of EBC coating, some coating materials penetrated into the stitching hole, resulting in a thin or loose EBC coating layer on the surface of the stitching hole of the specimen, and oxygen was easy to enter the stitching hole through the coating layer, resulting in local oxidation on the inner surface of the specimen stitching hole. The presence of the stitching hole weakens the oxidation resistance of the coating here, and oxygen enters through the stitching hole and reacts with the nearby fibers and matrix. During the tensile process, stress concentration occurs here and cracks occur. Due to oxidation reaction, the interface cannot release the energy at the crack tip, leading to the crack breaking through the fiber bundle, and the specimen would break here.

However, not all holes weaken the strength of the material. Matrix densification is an engineering problem in the preparation of large-thickness CMCs. It is difficult for matrix impregnation in large-thickness CMC materials, and the degree of matrix densification is quite low, leading to weak strength properties of the materials. Therefore, some researchers study micropore deposition technology, which processes a series of arrays of micro-holes (micro-hole diameters ranging from 0.1 to 1 mm) for large-thickness CMC components, and then deposits the matrix of CMC components. The influence of micro-holes on material strength can be reduced due to the small diameter of micro-holes and the avoidance of key positions of components during micro-holes machining. In addition, through the array of micro-holes, the matrix material can be effectively deposited along the micro-holes into the CMC components, which can effectively improve the degree of densification of CMCs, especially the degree of densification near the micro-holes is pretty high, which not only improves the overall degree of densification and strength performance of CMC components, but also eliminates the negative effect of micro-holes on strength.

4. Conclusions

In this paper, experimental studies on tensile mechanical properties of 2D plain-woven SiCf/SiC composites at room temperature and high temperature were carried out. The mechanical response characteristics and failure mechanism of the composites were revealed by combining fracture observation and

element analysis, and the factors affecting the strength properties of the materials were discussed in depth. The following conclusions can be drawn:

In high temperature environment, the reaction of asbestos with Si/Yb_2SiO_5/La_2O_3-Al_2O_3 environmental barrier coating will cause the coating to fall off. It is necessary to use alumina fiber felt with better high temperature resistance and stability as the thermal insulation filler to seal and keep heat in high temperature furnace.

Compared with the mechanical properties at room temperature, the tensile modulus and strength of SiCf/SiC composites at high temperature are lower, but the fracture strain increases and the toughness of the composites is enhanced. The mechanical properties of SiC materials at high temperature are related to the degree of inorganic. The inorganic degree of SiC materials at 1300˚C is higher, and the mechanical properties of SiC materials at 1350˚C are better than those at 1200˚C.

In 2D plain-woven composites, the strength of the material is weakened by the Z-direction stitching holes, which leads to the failure of the material easily at the cross-section with stitching holes. The reasons for the weakening of material properties are as follows: 1) Stitching holes destroy the continuity of local fibers and reduce the effective bearing area; 2) There is stress concentration at the edge of stitching hole, which is easy to be the crack source/failure source; 3) The presence of stitching holes accelerates the oxidation process of the matrix/fiber at the edge of holes and weakens the mechanical properties of the materials.

Acknowledgements

This work is supported by the National Natural Science Foundation of China [grant numbers U2241238], and the authors would like to acknowledge Postgraduate Innovation Special Fund Project of Jiangxi Province for funding this work through Project # YC2022-s734.

Conflicts of Interest

The authors declare no conflicts of interest regarding the publication of this paper.

References

[1] Naslain, R.R. (2005) SiC-Matrix Composites: Nonbrittle Ceramics for Thermo-Structural Application. *International Journal of Applied Ceramic Technology*, **2**, 75-84. http://doi.org/10.1111/j.1744-7402.2005.02009.x

[2] Padture, N.P. (2016) Advanced Structural Ceramics in Aerospace Propulsion. *Nature Materials*, **15**, 804-809. http://doi.org/10.1038/nmat4687

[3] Jiao, J. and Chen, M.W. (2014) New Generation of High-Temperature Material for Engine—Preparation, Property and Application of Ceramic Matrix Composites. *Aeronautical Manufacturing Technology*, **57**, 62-69.

[4] Kiser, J.D., Grady, J.E., Bhatt, R.T., Wiesner, V.L. and Zhu, D. (2016) Overview of CMC (Ceramic Matrix Composite) Research at the NASA Glenn Research Center.

[5] Luo, X., Xu, Y.L., Guo, X.J., *et al.* (2021) Research Progress of Ceramic Matric

Composites Turbine Rotors for Turbine Engines. *Journal of Propulsion Technology*, **42**, 230-240. http://doi.org/10.13675/j.cnki.tjjs.200156

[6] Zok, F.W. (2016) Ceramic-Matrix Composites Enable Revolutionary Gains in Turbine Engine Efficiency. *American Ceramic Society Bulletin*, **95**, 22-28.

[7] Liu, X.C., Xu, Y.L., Li, J., *et al.* (2022) Design, Fabrication and Testing of Ceramic-Matrix Composite Turbine Blisk. *Acta Materiae Compositae Sinica*, **40**, 1696-1706.

[8] Li, P., Wang, B.L., Zhen, W.Q. and Jiao, G. (2014) In-Plane Shear Properties of Plane-Woven SiC/SiC Composites. *Journal of Mechanical Strength*, **36**, 691-693. http://doi.org/10.16579/j.issn.1001.9669.2014.05.006

[9] Han, J.B., Wang, R.Q., Hu, D.Y., Liu, X., Zhang, L., Guo, X.J. and Cho, C. (2022) Multi-Scale Analysis and Experimental Research for Turbine Guide Vanes Made of 2D Braided SiCf/SiC Composites in High-Cycle Fatigue Regime. *International Journal of Fatigue*, **156**, Article ID: 106697. https://doi.org/10.1016/j.ijfatigue.2021.106697

[10] Wang, F., Teng, X.F., Hu, X.A., Jiang, Y., Guo, X.J., Li, L.B., Liu, X.C., Liu, X. and Lu, H.Y. (2022) Damage and Failure Analysis of a SiCf/SiC Ceramic Matrix Composite Using Digital Image Correlation and Acoustic Emission. *Ceramics International*, **48**, 4699-4709. http://doi.org/10.1016/j.ceramint.2021.11.006

[11] Morscher, G.N. (2004) Stress-Dependent Matrix Cracking in 2D Woven SiC-Fiber Reinforced Melt-Infiltrated SiC Matrix Composites. *Composites Science and Technology*, **64**, 1311-1319. https://doi.org/10.1016/j.compscitech.2003.10.022

[12] Wang, F., Teng, X., Jiang, Y., Hu, X., Lu, M., Guo, X., Liu, X., Liu, X. and Yu, D. (2022) Damage Analysis of a SiCf/SiC Ceramic Matrix Composite under Stepwise Fatigue Loading with Acoustic Emission. *Journal of the European Ceramic Society*, **42**, 4086-4097. http://doi.org/10.1016/j.jeurceramsoc.2022.04.027

[13] Song, J.Q., Wang, L.Y., Huang, J.T., Yang, H.Y., Huang, P., Luo, H., Wang, J.S., Zheng, K. and Luo, R.Y. (2022) Mechanical Behavior of 2D Woven SiCf/SiC Composites Investigated by Acoustic Emission and Digital Image Correlation. *Ceramics International*, **48**, 35340-35352. http://doi.org/10.1016/j.ceramint.2022.08.136

[14] Hu, D.-Y., Zeng, Y.-Q., Long, Z., Mei, W.-B., Shen, X.-L. and Wang, R.-Q. (2018) Effective Elastic Constants Prediction and Modal Test of 2D Braided SiC/SiC Ceramic Matrix Composites. *Journal of Propulsion Technology*, **39**, 465-472. http://doi.org/10.13675/j.cnki.tjjs.2018.02.028

[15] Zhang, D., Liu, Y., Liu, H., Feng, Y., Guo, H., Hong, Z., Chen, C. and Zhang, Y. (2021) Characterisation of Damage Evolution in Plain Weave SiC/SiC Composites Using *in Situ* X-Ray Micro-Computed Tomography. *Composite Structures*, **275**, Article ID: 114447. http://doi.org/10.1016/j.compstruct.2021.114447

[16] Dong, H., Gao, X., Zhang, S., Song, Y., Yang, J. and Wang, F. (2022) Effects of Heat Treatment on the Mechanical Properties at Elevated Temperatures of Plain-Woven SiC/SiC Composites. *Journal of the European Ceramic Society*, **42**, 412-419. http://doi.org/10.1016/j.jeurceramsoc.2021.10.027

[17] Hong, Z., Yue, X., Wang, Z., Wen, Z., Zhang, Y., Li, Z., Ai, C., Wang, P., Zhang, X. and Yue, Z. (2021) Mechanical Properties Degradation and Microstructure Evolution of 2D-SiCf/SiC Composites in Combustion Gas Environment. *Journal of the European Ceramic Society*, **41**, 6845-6858. http://doi.org/10.1016/j.jeurceramsoc.2021.07.026

[18] Bansal, N.P. and Lamon, J. (2015) Ceramic Matrix Composites: Materials, Modeling and Technology. John Wiley & Sons Inc. https://doi.org/10.1002/9781118832998

[19] Grady, J.E. (2013) CMC Technology Advancements for Gas Turbine Engine Applications.